

# HENRY

Hydraulic Engineering Repository

Ein Service der Bundesanstalt für Wasserbau

---

Conference Paper, Published Version

## **Ungewitter, Christian; Kauther, Regina; Lempp, Christof** **A contribution on the unusual behaviour in the stress-strain-relationship of mudrocks**

---

Verfügbar unter/Available at: <https://hdl.handle.net/20.500.11970/107597>

Vorgeschlagene Zitierweise/Suggested citation:

Ungewitter, Christian; Kauther, Regina; Lempp, Christof (2020): A contribution on the unusual behaviour in the stress-strain-relationship of mudrocks. In: Marcher; Thomas (Hg.): Beiträge zum 1. Hard Soil - Soft Rock (HSSR) Minisymposium, 27 Nov 2020, Graz. Graz: Technische Universität Graz. S. 137-152.

### **Standardnutzungsbedingungen/Terms of Use:**

Die Dokumente in HENRY stehen unter der Creative Commons Lizenz CC BY 4.0, sofern keine abweichenden Nutzungsbedingungen getroffen wurden. Damit ist sowohl die kommerzielle Nutzung als auch das Teilen, die Weiterbearbeitung und Speicherung erlaubt. Das Verwenden und das Bearbeiten stehen unter der Bedingung der Namensnennung. Im Einzelfall kann eine restriktivere Lizenz gelten; dann gelten abweichend von den obigen Nutzungsbedingungen die in der dort genannten Lizenz gewährten Nutzungsrechte.

Documents in HENRY are made available under the Creative Commons License CC BY 4.0, if no other license is applicable. Under CC BY 4.0 commercial use and sharing, remixing, transforming, and building upon the material of the work is permitted. In some cases a different, more restrictive license may apply; if applicable the terms of the restrictive license will be binding.

# A contribution on the unusual behaviour in the stress-strain-relationship of mudrocks

Ungewitter<sup>1)</sup>, Kauther<sup>1)</sup>, Lempp<sup>2)</sup>

<sup>1)</sup> Bundesanstalt für Wasserbau, Karlsruhe

<sup>2)</sup> Martin-Luther-Universität, Halle (Saale)

**Abstract.** In the course of an extensive triaxial testing campaign on four different slaking rocks from Germany it was found that the stress-strain curves show a characteristic inflection point, which could not be explained directly. Former studies on this subject supposed the influence of the pore pressure (Bundesanstalt für Wasserbau, 1983) or the reaching of the elastic limit state (Popp & Salzer, 2007) without any further systematic research. Another possible influence could be the maximum burial depth.

In order to investigate the stress-strain behaviour in detail consolidated drained and undrained triaxial tests were evaluated. The influence of the maximum burial depth can be ruled out because no correlation or other relationship between the burial depth and the differential stress at the inflection point could be found. Pore pressure- and pore volume-curves show that the inflection point is caused by dilatancy at high pore pressures generated by high shearing rates in relation to the low permeability of the mudrocks.

Due to the high shearing rate a pore pressure arises inside the specimen counteracting the increase of the effective differential stress. Therefore, the effective stress is reduced and the matrix of the rock is weakened causing new cracks or the growth of existing ones and creating new pore volume. Pore water can flow into the cracks and the pore pressure around the cracks decreases. The effective pressures increase again which is displayed in stress-strain curves by the inflection point.

Consequently, the inflection point is a dilatancy effect accompanied by pore pressure changes and becomes apparent by the interplay between very low permeabilities and a stiffness ranging between hard soil and rock. These findings have an impact on the geotechnical and laboratory investigation of mudrocks because the inflection point marks the onset of cracking events inside the rock.

**Key words:** mudrock; inflection point; stress-strain behaviour; excess pore water pressure; dilatancy

# 1 Introduction

Slaking rocks like mudrock are exposed over large areas in Germany and Europe. Therefore, these rocks play a crucial role in many infrastructure projects. Despite their abundance the research on slaking rocks was limited in the past. However, in the last two decades there has been a growing interest in this geomaterial, especially with regard to the construction of nuclear waste disposals, the exploitation of shale gas resources and the role of mudrocks as a barrier for CO<sub>2</sub> storage technologies.

In this paper the term slaking rock is used in accordance with Lempp (1979) and Nickmann (2010): Slaking rocks form a group of geomaterial whose strength is substantially reduced by hydraulic-mechanical disintegration mechanisms within a relatively short period of time (days to a few months) resulting in the formation of loose rock. The disintegration is not reversible and can be caused by a single wet-dry change.

An extensive triaxial testing campaign on the influence of different sampling and storing procedures on the strength of slaking rocks (Lower Aalenian clay [Opalinus clay], Hauterivian mudrock, Cretaceous marl, Triassic siltstone) was carried out. It was found that the stress-strain curves of the Opalinus clay and the Hauterivian mudrock show a characteristic inflection point (see Fig. 1).

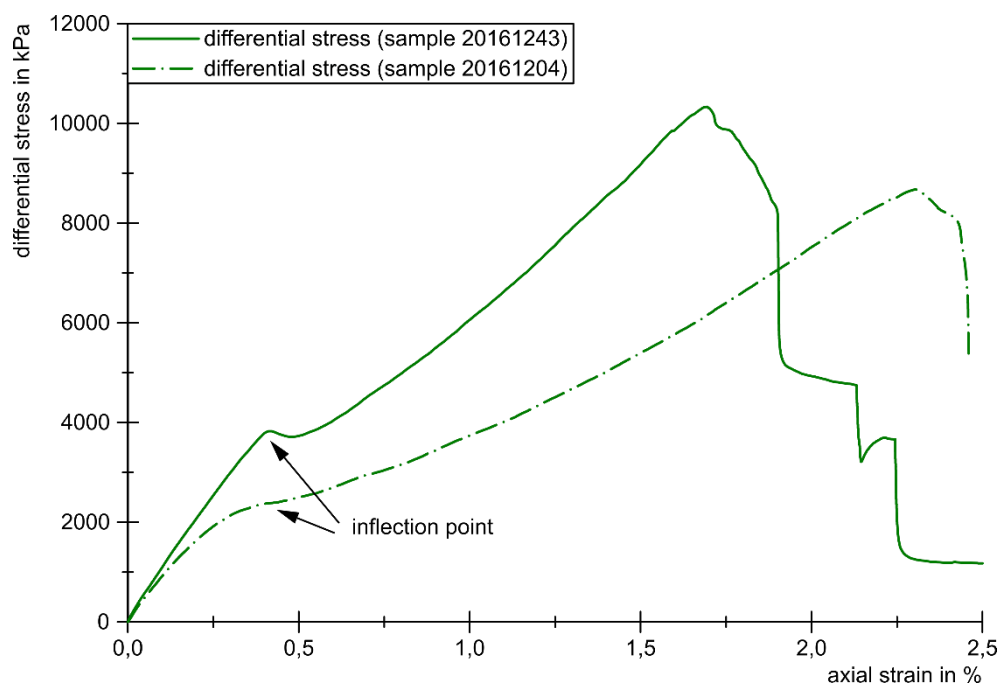


Fig. 1: Stress-strain curves of two Hauterivian mudrock samples

This inflection point is also apparent in studies e. g. of Wichter & Gudehus (1982) and the Institut für Gebirgsmechanik (2008) but without giving an explanation. Other studies dealing with the inflection point only placed suggestions for its

development like the influence of the pore pressure (Bundesanstalt für Wasserbau, 1983) or the reaching of the elastic limit state (Popp & Salzer, 2007). So, the question remains: What causes the development of the characteristic inflection point in the stress-strain curves of certain slaking rocks?

## 2 Sampling and testing procedure

The Hauterivian mudrock, Triassic siltstone and Cretaceous marl were drilled with a wireline coring tool equipped with a pilot drill bit according to DIN EN ISO 22475-1 (Deutsches Institut für Normung, 2007). After the recovery the liners were stored in a room with constant temperature and humidity until the transport to the Federal Waterways Research and Engineering Institute (Bundesanstalt für Wasserbau) in Karlsruhe. The Opalinus clay was block-sampled from the Boßlertunnel near Kirchheim unter Teck.

After the arrival in the laboratory the liner samples were described according to DIN EN ISO 14689 (Deutsches Institut für Normung, 2018). All rocks were tested for their slaking behaviour according to the procedure of Nickmann (2010) and showed a medium to very high proneness for slaking behaviour. Then, suitable specimens were chosen for further testing. The preparation of the slaking rock samples prior to testing is described in Günther et al. (2017).

After the preparation the samples were placed in the triaxial testing system. The triaxial tests were conducted in a soil mechanical framework with stages of saturation, consolidation and shearing including the measurement of the pore water pressure (see Fig. 2).

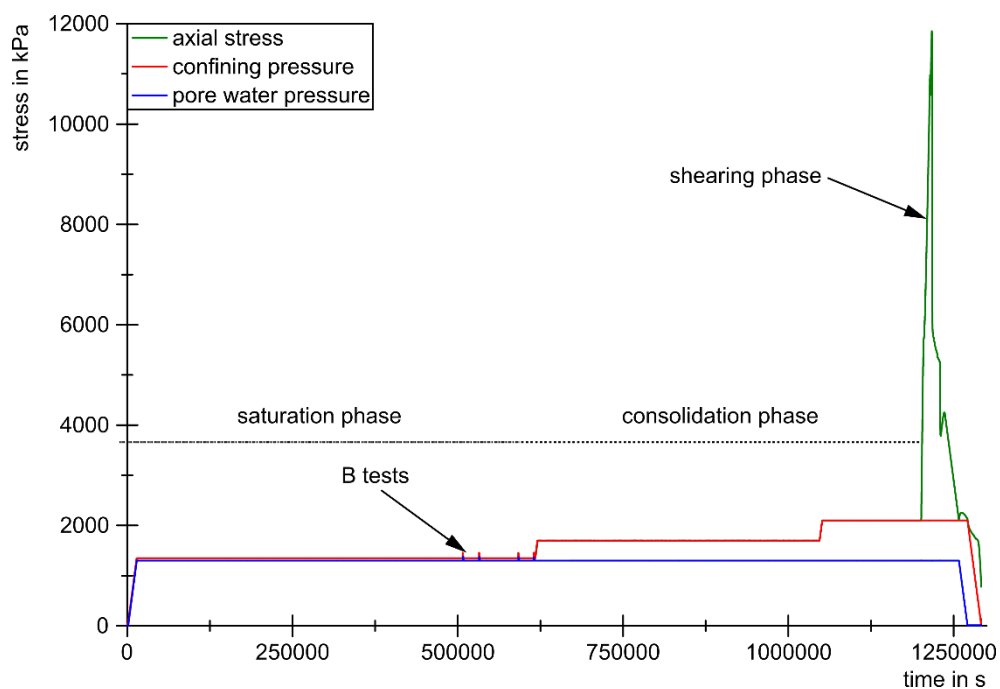


Fig. 2: Procedure of a triaxial test conducted in this study (CD-test as an example)

In the saturation phase a back pressure of 1300 kPa was applied for all tests. During the saturation B-tests were conducted to check the saturation of the specimen. In the consolidation stage, the axial pressure and confining pressure were increased to 1700 kPa. Therefore, the effective stress acting on the samples was 400 kPa reflecting the calculated in situ stress. When the first stage of the consolidation is finished the stresses are increased a second time to a level where the specimen will be sheared. Before shearing until failure, it is obligatory to wait for the end of the second consolidation stage.

### 3 Results

In Fig. 3 the stress-strain curves and pore water pressure curves from consolidated-undrained triaxial tests of slaking rocks with an inflection point are shown (Hauterivian mudrock, Opalinus clay). With the beginning of the shearing phase the pore water pressure increases with the axial stress. The point where the pore water pressure reaches its maximum (Opalinus clay) or a plateau (Hauterivian mudrock) approximately corresponds to the inflection point. Hence, there is possibly a link between the generation of excess pore water pressure and the origin of the inflection point which will be discussed in the next chapter. The inflection point also occurs in consolidated-drained tests which will also be discussed in the next chapters.

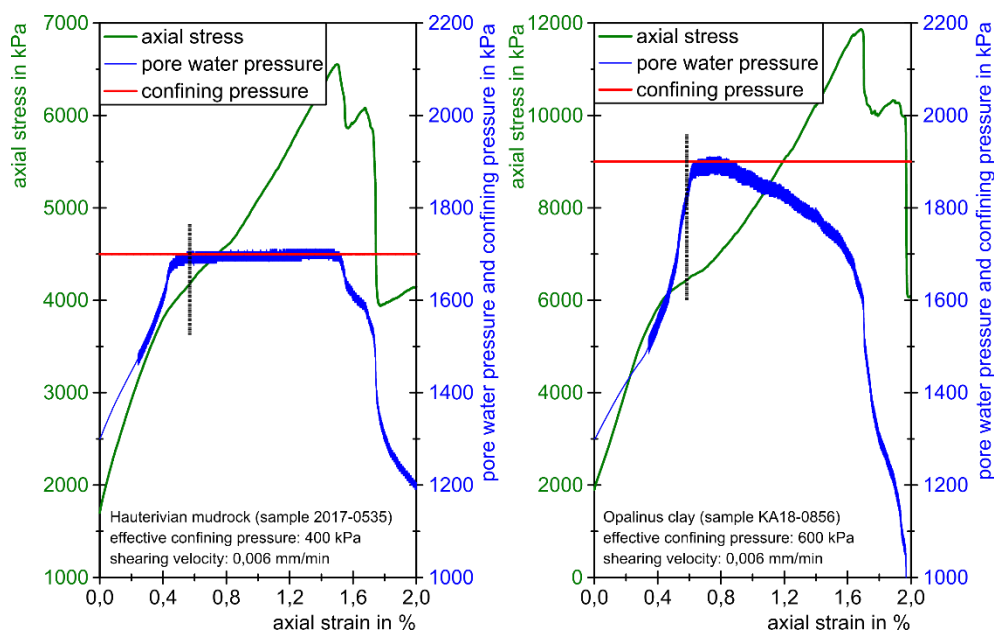


Fig. 3: Slaking rocks under investigation with inflection point

In Fig. 4 the stress-strain curves and pore water pressure curves of slaking rocks without an inflection point are shown. For the Cretaceous marl a consolidated-drained test was performed. Thus, the pore water pressure was kept constant and is not shown in Fig. 4. The pore water pressure of the Triassic siltstone (consolidated-undrained test) increases until reaching the confining pressure. But

there is no inflection point apparent as well as for the Cretaceous marl. The reason for this apparently contradictory behaviour will be discussed in chapter 4.

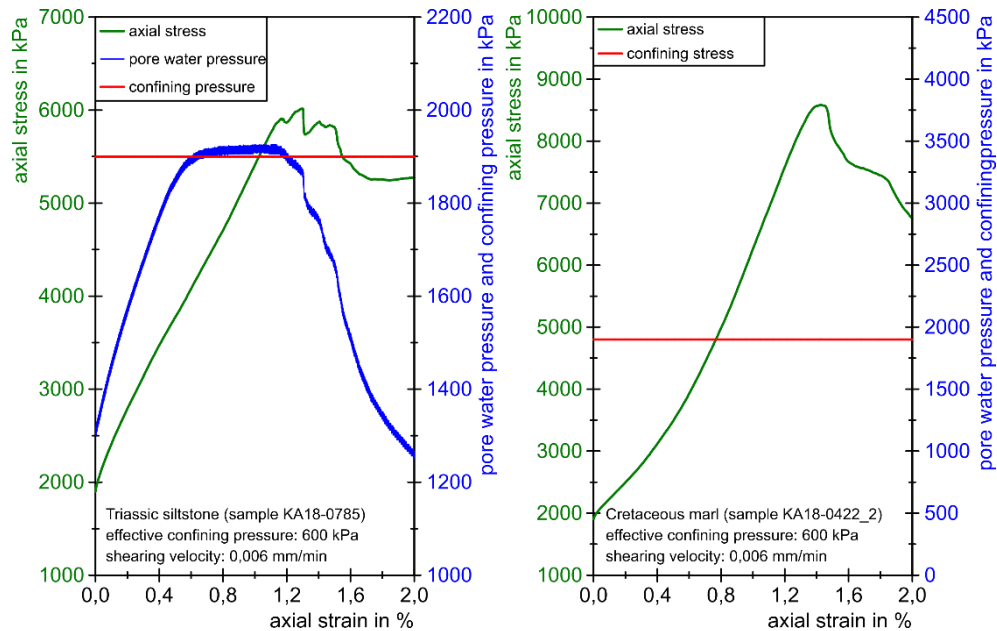


Fig. 4: Slaking rocks under investigation without inflection point

## 4 Discussion

The link between the pore water pressure and the inflection point becomes clearer in Fig. 5 where stress-strain curves and change in pore volume-strain curves from consolidated-drained triaxial tests of Hauterivian mudrock samples are shown. The model of the reconstructed process during the shearing phase can be subdivided in three phases (A, B, C). In Phase A the axial stress is increased, the pore water pressure rises resulting in a parabolic distribution of the pore water pressure inside the specimen (green curve). The pore water drains out of the sample (blue arrows). The pore water pressure reaches its highest value in the middle of the specimen lowering the effective stresses and thus weakening the sample. This results in the generation of new micro cracks and in the growth and coagulation of existing ones. New crack volume is generated (phase B) producing a local suction pressure. A part of the pore water flows into the new crack spaces resulting in flatter pore volume curves because less pore water drains of the sample. This is also the point where the pore water pressure in undrained tests reaches its maximum value. In the case of the Hauterivian mudrock the maximum of the pore water pressure is limited by the value of the confining pressure (see Fig. 3). If the pore water pressure reaches the value of the confining pressure it cannot increase any further. As a result, the growth and coagulation of micro cracks stops. Therefore, no additional pore water can flow into the cracks and is forced to drain out of the sample resulting in a steeper change in pore volume curve (phase C).

The formation of the inflection point indicates undrained behaviour of the mudrock sample even when the test is performed with open pore water lines (drained).

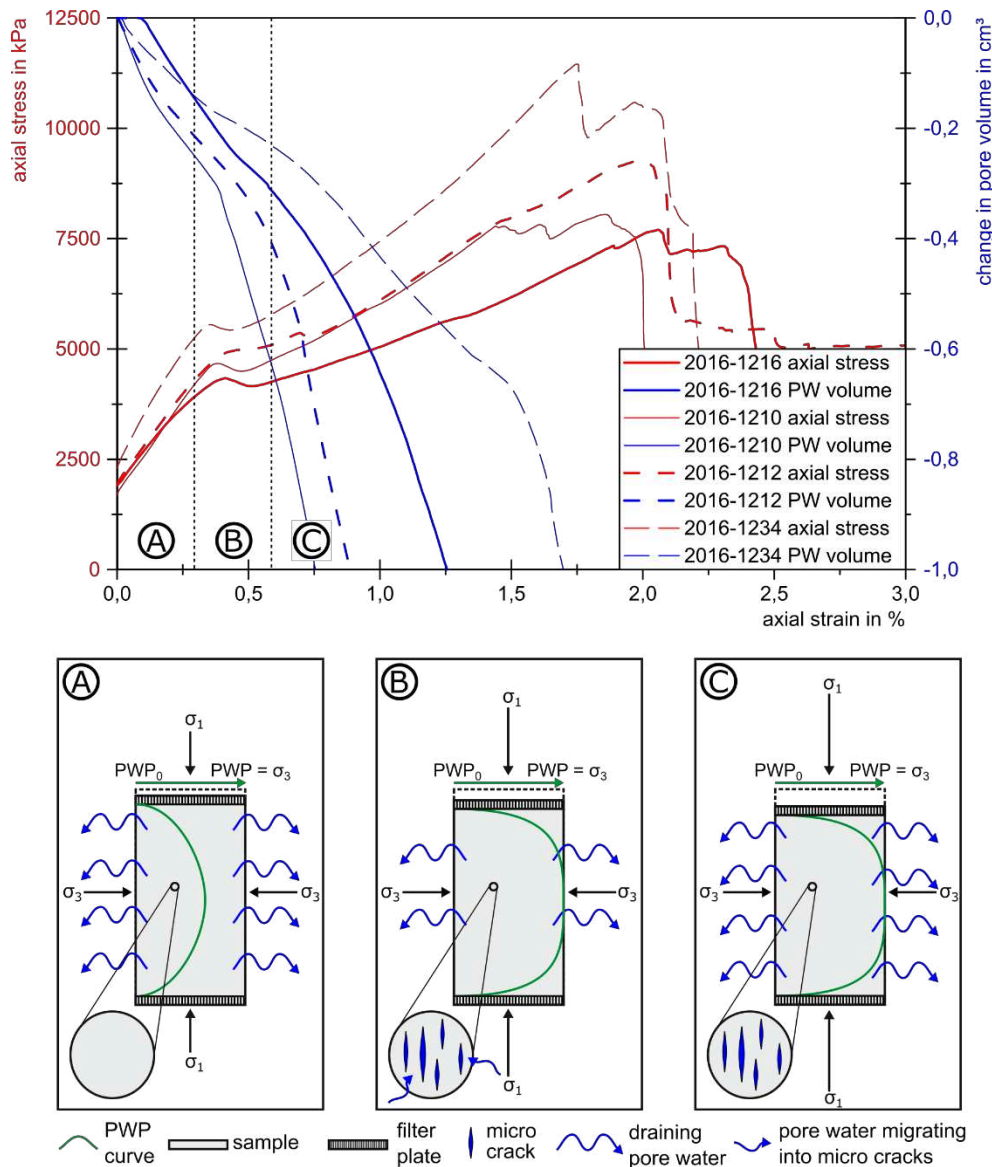


Fig. 5: Model of the hydro-mechanical processes in the course of the inflection point

The description of the processes in Fig. 5 is supported by the diagrams shown in Fig. 6. The left diagram depicts a consolidated-drained triaxial test performed by the authors. The right diagram shows a uniaxial compression test with radial strain measurement performed by the Institut für Gebirgsmechanik GmbH (2008). Basically, both diagrams show increasing volumetric and radial strains when the inflection point sets in. In the left diagram the curve of the change in cell volume becomes steeper around the inflection point. In the right diagram the radial strain increases when the inflection point is reached. Both observations can be explained by the generation of new micro cracks or growth and coagulation of existing ones parallel to the load direction resulting in accelerated radial deformation.



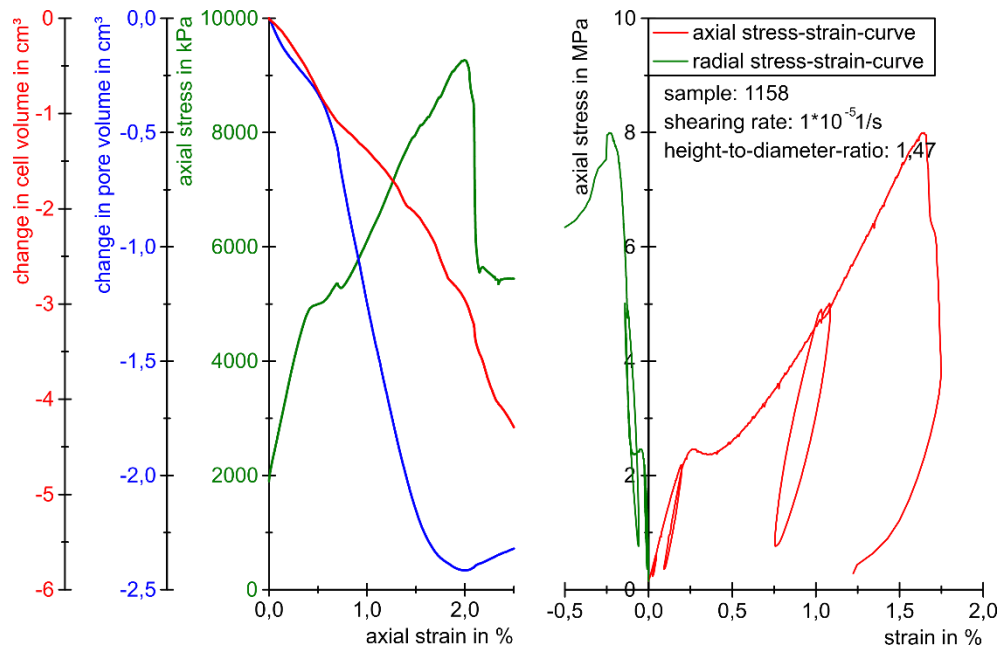


Fig. 6: Increasing strains around the inflection point (Hauterivian mudrock sample)

A remarkable feature is the decrease of the modulus (slope of the stress-strain curve) after the inflection point (see Fig. 1). Fig. 7 shows the ratios between the modulus of elasticity prior to the inflection point and the modulus after the inflection point. These ratios resemble typical ratios between drained and undrained modulus of elasticity of geomaterials shown in Tab. 1 where the undrained modulus is higher than the drained modulus.

This can be explained by the flow of pore water into the newly developed crack space causing locally drained conditions around the cracks during shearing. Prior to the inflection point undrained conditions prevail inside the mudrock sample. After the occurrence of the inflection point the newly developed micro cracks act as an additional drainage causing decreasing drainage lengths inside the sample (see Fig. 7:  $a > b$ ). Thus, around the future shear zone drained conditions prevail which is reflected by the ratio between the modulus of elasticity prior to the inflection point and the modulus after the inflection point (cf. Fig. 7 and Tab. 1).

In summary the development of the inflection point can be described in the following way: The pore water pressure increases during loading. At the same time the effective stress inside the sample decreases weakening the structure and leading to the formation of new micro cracks or the growth and coagulation of existing ones. This results in an increased radial and axial deformation. At the same time local suction pressures occur. The pore water flows into the micro cracks. Thus, the pore water pressure decreases and the effective stress increases resulting in a rising progression of the stress-strain curve.



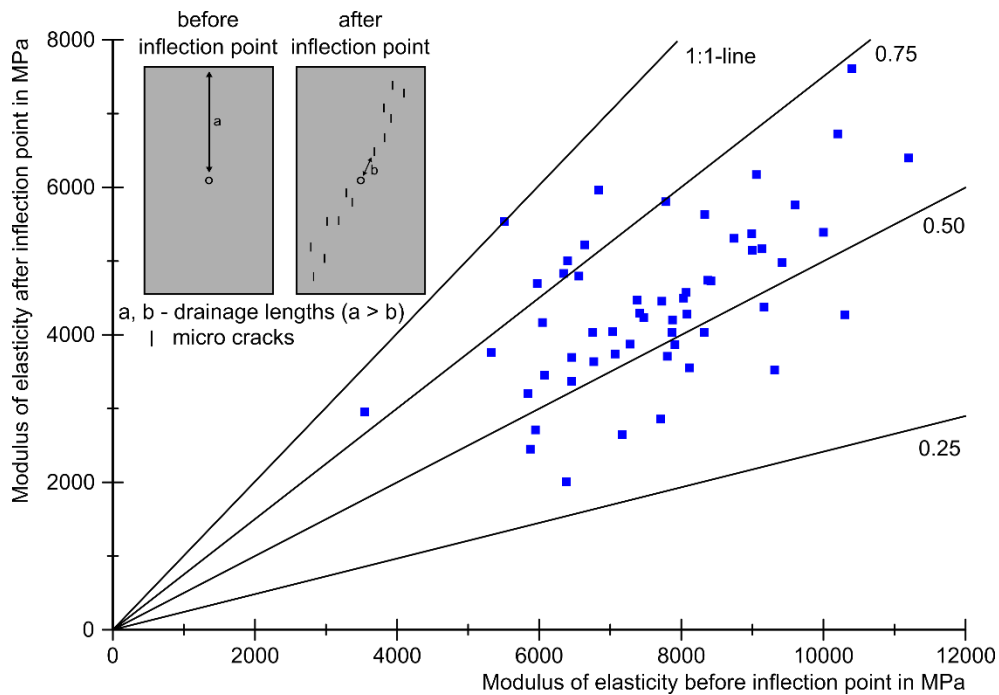


Fig. 7: Relationship of the modulus of elasticity prior to the inflection point and the modulus after the inflection point from samples of the Hauterivian mudrock, black lines mark the ratio between the modulus of elasticity prior to the inflection point and the modulus after the inflection point, the schematic sketches (top right) show the reduction of the drainage length prior to and after the inflection point

Tab. 1: Compilation of drained and undrained the modulus of elasticity of different rocks

Publication, rock	$E_d$ in GPa ( $\sigma'_3$ in MPa)	$E_u$ in GPa ( $\sigma'_3$ in MPa)	ratio $E_d/E_u$
Islam & Skalle (2013), Pierre I shale	0,64 (17)	1,36 (20)	0,47
Makhnenko & Labuz (2016), Barea sandstone	10,00 (5) 10,70 (5)	14,90 (5) 15,70 (5)	0,67 0,68
Giger et al. (2018), Opalinus clay	5,00 (18,4) 2,00 (6,4)	5,10 (18,1) 3,10 (3,3)	0,98 0,65
Wild & Amann (2018), Opalinus clay	0,68 (2,01) 0,51 (0,76)	1,49 (1,98) 1,15 (0,76)	0,45 0,44

Now the question arises what properties of slaking rocks contribute to the formation of the inflection point and why only some slaking rocks show this behaviour. As already shown in Fig. 3 and Fig. 4 it is apparent that the inflection point occurs for samples of the Opalinus clay and the Hauterivian mudrock, but not for the Triassic siltstone and the Cretaceous marl. The next paragraphs will deal with the permeability, stiffness and anisotropy of the slaking rocks.

In Tab. 2 the permeability of rocks similar to those investigated in this study is listed. The permeability of mudrocks varies between  $1,0 \cdot 10^{-13}$  and  $1,3 \cdot 10^{-14}$  m/s. This is two to four orders of magnitude less than marl and siltstone. Rocks with a higher permeability have a better ability to drain. Thus, the pore water pressure under load will not increase as strongly as in mudrocks. The better drainage process prevents the development of micro cracks, the dilation of the rock and thus the development of the inflection point.

Tab. 2: Permeability of different slaking rocks

Rock (source)	Permeability in m/s
Emscher marl (CDM Smith, 2016)	$5,0 \cdot 10^{-10}$
Marl of the Freshwater Molasse (Keller, et al., 1990)	$1,0 \cdot 10^{-10}$
Marl of the Freshwater Molasse (Dollinger, 1997)	$4,6 \cdot 10^{-10}$
Siltstone (Domenico & Schwartz, 1997)	$1,0 \cdot 10^{-10} - 1,4 \cdot 10^{-8}$
Siltstone (Singhal & Gupta, 1999)	$1,0 \cdot 10^{-12} - 1,4 \cdot 10^{-10}$
Callovo-oxfordian clay (Jougnot, et al., 2010)	$1,3 \cdot 10^{-14}$
Callovo-oxfordian clay (Gens, et al., 2007)	$1,0 \cdot 10^{-13} - 5,0 \cdot 10^{-13}$
Opalinus clay (Keller & Holzer, 2018)	$3,8 \cdot 10^{-14}$

The difference of the stiffness values between the mudrocks and the marl and siltstone are less pronounced than the difference in permeability differing by the factor of two to three (see Tab. 3). To generate an inflection point in the stress-strain curve the stiffness of a rock has to be so high that brittle fractures are possible to induce a dilatant behaviour during shearing. All rocks investigated in this study showed brittle failure after reaching their peak strength. Therefore, the stiffness of the slaking rocks alone cannot explain the occurrence or the absence of the inflection point. The influence of the stiffness in the range of the investigated rocks on the formation of the inflection point is not obvious. Thus, the permeability is regarded as the more important influence on the formation of the inflection point.

Tab. 3: Stiffness of the rocks investigated in this study in MPa (determined for the Hauterivian mudrock and the Opalinus clay from the linear section of the stress-strain curve prior to the inflection point, for the Triassic siltstone and Cretaceous marl from the linear section of the stress-strain curve);  $\sigma'_3$ : 200 to 800 kPa

Rock	Arithmetic mean $\pm$ standard deviation; number of tests
Hauterivian mudrock	$7584 \pm 1592$ MPa; n = 70
Triassic siltstone	$3223 \pm 1177$ ; n = 10
Opalinus clay	$7864 \pm 2379$ ; n = 5
Cretaceous marl	$2697 \pm 771$ ; n = 4

The influence of the anisotropy on the formation of the inflection point is shown in Fig. 8. Perpendicular to the bedding the inflection is apparent (see Fig. 3). For measurements parallel to the bedding of Wichter & Gudehus (1982) with Opalinus clay and of the authors with Hauterivian mudrock the inflection point is less

obvious with other characteristics (see Fig. 8). The inflection point sets in earlier and is less pronounced while the reaction of the pore water volume curve is more pronounced. When the load is applied parallel to the bedding the layering of the clay minerals acts as a kind of predetermined breaking point. This causes an early development of micro cracks along the layering of the clay minerals leading to an early set in of the inflection point. Thus, the anisotropy is an important influence on the characteristics of the inflection point.

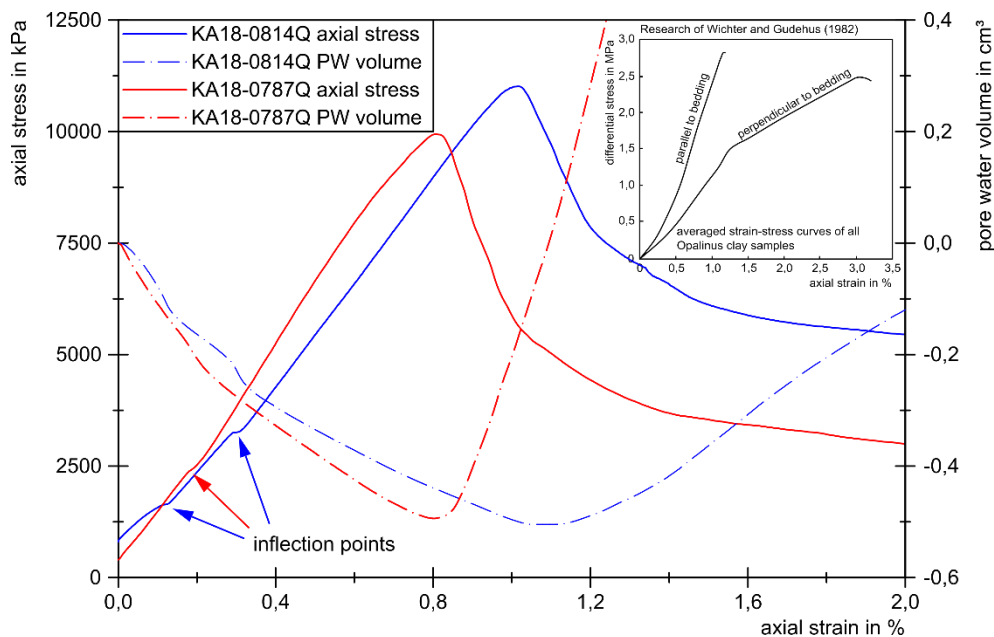


Fig. 8: Influence of the anisotropy on the inflection point of Hauterivian mudrock samples loaded parallel to the bedding; top right: Results of a triaxial testing campaign on Opalinus clay (Wichter & Gudehus, 1982)

The findings on the origin of the inflection point (excess pore water pressure and dilatancy) have direct impact on a dilatancy model for mudrock including thresholds for the formation of micro cracks developed by Jobmann et al. (2015). According to this model the first micro cracks develop at a differential stress half the peak differential stress of a mudrock. But it is stated in the report that the “micro crack threshold” has to be investigated for every single mudrock formation. Comparing this definition with the findings in this study (see Fig. 9) it is evident that the threshold is too high for the Hauterivian mudrock and must be revised to a lower value. The histogram shows that the threshold should be 0.4-fold of the maximum differential stress when considering the maximum count of samples per class. If there shall be no major micro crack development at all the threshold must be lowered to the 0.25-fold of the maximum differential stress.

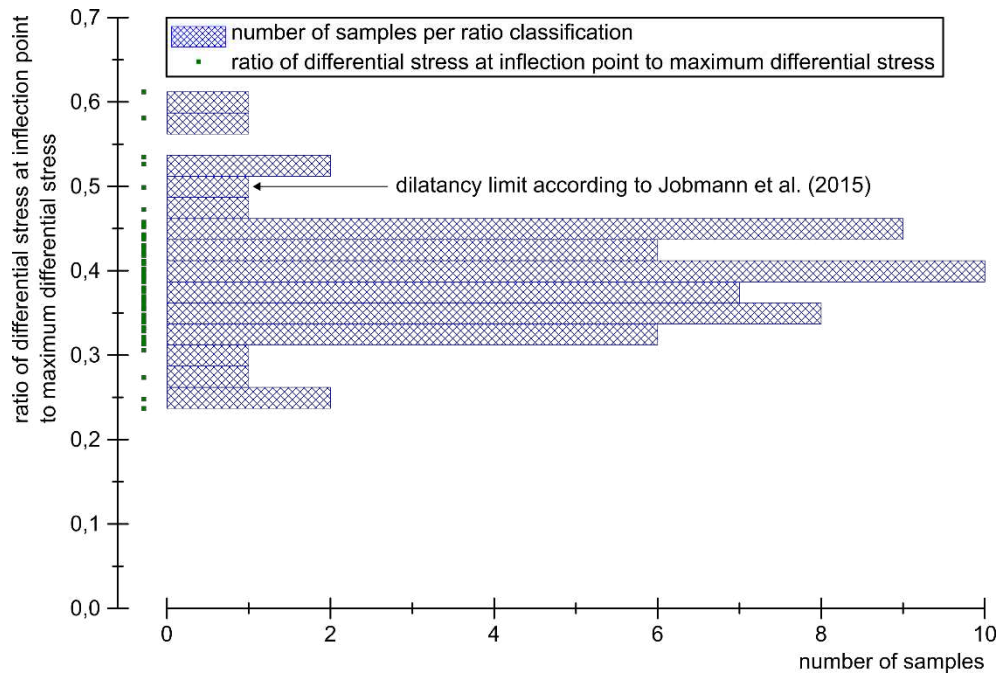


Fig. 9: Histogram of the ratio of differential stress at inflection point to maximum differential stress from the Hauterivian mudrock

## 5 Conclusion

The factors influencing the inflection point are shown in Fig. 10. The inflection point is mainly caused by excess pore water pressure and the dilatancy. Its shape and characteristic are influenced by the stiffness and permeability of the slaking rocks and its anisotropy. The presence of the inflection point in stress-strain curves of mudrocks is rooted in its unique combination of a relatively high stiffness compared to clayey soil, very low permeability and pronounced anisotropy. This unique combination of properties places the slaking rocks between soil and hard rock and should be considered as a separate geomaterial group.

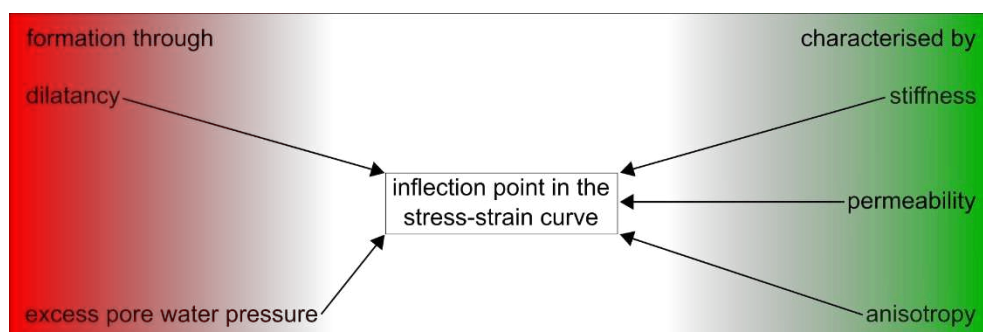


Fig. 10: Influences on the formation of the inflection point

The occurrence of the inflection point has direct implications on geotechnical laboratory procedures and the definition of characteristic values extracted from triaxial tests. The inflection point originates from excess pore water pressure due

to too high shearing rates. This has to be considered when defining characteristic values from the results of the triaxial test. When there are indications for excess pore water pressure generation then undrained conditions prevail inside the specimen. Thus, the results of the triaxial test reflect undrained behaviour even if the triaxial test was conducted with consolidated-drained boundary conditions.

## 6 Literature

- Bundesanstalt für Wasserbau, 1983. *Ausbau des Mittellandkanals für das 1350-t-Schiff: Baugrund und Gründung der Brücke Nr. 159 bei km 120,100*, Karlsruhe: Bundesanstalt für Wasserbau.
- CDM Smith, 2016. *Gelsenkirchen, Sellmannsbach, Bau des Abwasserkanals einschl. Mischwasserbehandlung von km 0,00 bis km 5,16 und Bau der Druckrohrleitung - Baugrundgutachten und Bodenmanagementkonzept*, s.l.: s.n.
- Deutsches Institut für Normung, 2007. *DIN EN ISO 22475-1:2007-01: Geotechnische Erkundung und Untersuchung - Probenentnahmeverfahren und Grundwassermessungen - Teil 1: Technische Grundlagen der Ausführung*. Berlin: Beuth-Verlag.
- Deutsches Institut für Normung, 2018. *DIN EN ISO 14689:2018-05: Geotechnische Erkundung und Untersuchung - Benennung, Beschreibung und Klassifizierung von Fels*. Berlin: Beuth-Verlag.
- Dollinger, J., 1997. *Geologie und Hydrogeologie der Unteren Süßwassermolasse im SBB-Grauholztunnel bei Bern*, Bern: Bundesamt für Umwelt, Wald und Landschaft.
- Domenico, P. A. & Schwartz, F. W., 1997. *Physical and Chemical Hydrogeology*. 2 ed. New York: Wiley.
- Gens, A., Vaunat, J., Garitte, B. & Wileveau, Y., 2007. In situ behaviour of a stiff layered clay subject to thermal loading - Observations and interpretation. *Géotechnique*, Volume 57/2, p. 207–228.
- Giger, S. B. et al., 2018. Consolidated-undrained triaxial testing of Opalinus Clay: Results and method validation. *Geomechanics for Energy and the Environment*, Volume 14, p. 16–28.
- Günther, C., Kauther, R. & Lempp, C., 2017. Ein Workflow zur Untersuchung effektiver Festigkeitsparameter veränderlich-fester Gesteine. In: *Fachsektionstage Geotechnik - Interdisziplinäres Forum: Tagungsband*. Würzburg: Deutsche Gesellschaft für Geotechnik, p. 276–281.

- Institut für Gebirgsmechanik GmbH, 2008. *Durchführung von Felsmechanischen Untersuchungen an tertiärem Tonstein aus Bohrungen für das Projekt „Neubau Weserschleuse Minden“*, Leipzig: s.n.
- Islam, M. A. & Skalle, P., 2013. An Experimental Investigation of Shale Mechanical Properties Through Drained and Undrained Test Mechanisms. *Rock Mechanics and Rock Engineering*, Volume 46/6, p. 1391–1413.
- Jobmann, M., Maßmann, J., Meleshyn, A. & Polster, M., 2015. *Projekt ANSICHT - Quantifizierung von Kriterien für Integritätsnachweise im Tonstein*, Peine: Deutsche Gesellschaft zum Bau und Betrieb von Endlagern für Abfallstoffe.
- Jougnot, D., Revil, A., Lu, N. & Wayllace, A., 2010. Transport properties of the Callovo-Oxfordian clay rock under partially saturated conditions. *Water Resources Research*, Volume 46/8, p. W08514.
- Keller, B. et al., 1990. *Sedimentäre Architektur der distalen Unteren Süßwassermolasse und ihre Beziehung zur Diagenese und der Petrophysik. Eigenschaften am Beispiel der Bohrungen Langenthal*, Wettingen: Nationale Genossenschaft für die Lagerung radioaktiver Abfälle.
- Keller, L. M. & Holzer, L., 2018. Image-Based Upscaling of Permeability in Opalinus Clay. *Journal of Geophysical Research: Solid Earth*, Volume 123, p. 1–11.
- Lempp, C., 1979. *Die Entfestigung überkonsolidierter, pelitischer Gesteine Süddeutschlands und ihr Einfluss auf die Tragfähigkeit des Straßenuntergrundes*. Tübingen: Eberhard-Karls-Universität.
- Makhnenko, R. Y. & Labuz, J. F., 2016. Elastic and inelastic deformation of fluid-saturated rock. *Philosophical Transactions of the Royal Society A: Mathematical, Physical and Engineering Sciences*, Volume 374, p. 1–22.
- Nickmann, M., 2010. *Abgrenzung und Klassifizierung veränderlich fester Gesteine unter ingenieurgeologischen Aspekten*. München: Pfeil Verlag.
- Popp, T. & Salzer, K., 2007. Anisotropy of seismic and mechanical properties of Opalinus clay during triaxial deformation in a multi-anvil apparatus. *Physics and Chemistry of the Earth, Parts A/B/C*, Volume 32/8-14, pp. 879-888.
- Singhal, B. B. S. & Gupta, R. P., 1999. *Applied hydrogeology of fractured rocks*. 1 ed. Dordrecht: Springer.
- Wichter, L. & Gudehus, G., 1982. Ergebnisse von Biaxial- und Triaxialversuchen am Opalinuston. *Geotechnik*, Volume 5/2, pp. 74-82.
- Wild, K. & Amann, F., 2018. Experimental study of the hydro-mechanical response of Opalinus Clay – Part 1: Pore pressure response and effective geomechanical

properties under consideration of confinement and anisotropy. *Engineering Geology*, Volume 237, p. 32–41.